Development 129, 5487-5498

doi:10.1242/dev.00148

Drosophila Regulatory factor X is necessary for ciliated sensory neuron differentiation

Raphaelle Dubruille[1,*], Anne Laurençon[1,*], Camille Vandaele[1,*], Emiko Shishido[2], Madeleine Coulon-Bublex[1], Peter Swoboda[3], Pierre Couble[1], Maurice Kernan[2] and Bénédicte Durand[1,†]

[1]Centre de Génétique Moléculaire et Cellulaire, CNRS UMR-5534, Université Claude Bernard Lyon-1, 69622 Villeurbanne, France
[2]Department of Neurobiology and Behavior, The State University of New York at Stony Brook, Stony Brook, New York 11794, USA
[3]Karolinska Institute, Department of Biosciences, Södertörn University College, Section of Natural Sciences, S-14189 Huddinge, Sweden

*These authors contributed equally to this work
†Author for correspondence (e-mail: durand-b@univ-lyon1.fr)

Accepted 3 September 2002

SUMMARY

Ciliated neurons play an important role in sensory perception in many animals. Modified cilia at dendrite endings serve as sites of sensory signal capture and transduction. We describe *Drosophila* mutations that affect the transcription factor RFX and genetic rescue experiments that demonstrate its central role in sensory cilium differentiation. *Rfx* mutant flies show defects in chemosensory and mechanosensory behaviors but have normal phototaxis, consistent with *Rfx* expression in ciliated sensory neurons and neuronal precursors but not in photoreceptors. The mutant behavioral phenotypes are correlated with abnormal function and structure of neuronal cilia, as shown by the loss of sensory transduction and by defects in ciliary morphology and ultrastructure. These results identify *Rfx* as an essential regulator of ciliated sensory neuron differentiation in *Drosophila*.

Key words: Ciliated sensory neuron, RFX, *Drosophila*

INTRODUCTION

In multicellular organisms, sensory perception relies on cells with specialized sensory structures. In many sense organs these structures are modified cilia: vertebrate examples include the outer segments of the retinal and pineal photoreceptors, the kinocilia associated with the stereocilia of the hair cells and the multiple cilia on the sensory neurons in the main olfactory epithelium. In invertebrates, chemosensory sensilla and many mechanosensory organs, but not photoreceptors, are innervated by ciliated neurons (Eakin, 1972).

Cilia are found in most eukaryotes except for fungi and higher plants. They are distinguished by an axoneme, a radially symmetric cytoskeleton of nine microtubule doublets and associated structures, enclosed in an extension of the plasma membrane. The presence or absence of a central microtubule pair classifies cilia into two types. Those with a central pair (9+2 configuration) usually have a propulsive function, while those without a central microtubule pair (9+0 configuration) are found on many animal cell types, where they are known as 'primary' cilia. Some 9+0 cilia [e.g. those on the mammalian embryonic node (Nonaka et al., 1998)], move with a circular, whirling motion. Sensory cilia are derived from primary cilia and have been modified to varying degrees; most are probably non-motile.

The importance of cilia for sensory transduction has been demonstrated in the nematode *C. elegans*, in which mutations affecting ciliary structure have been isolated in screens for a variety of sensory defects. These include defective osmotic avoidance (*Osm*), chemotaxis (*Che*), dauer formation (*Daf*) as well as defective fluorescent dye uptake (*Dyf*) and poor male mating behavior (Perkins et al., 1986; Starich et al., 1995).

In *Drosophila*, nonvisual sensory perception relies on two major classes of sense organs. Type I organs or sensilla include one or more neurons and several support cells that construct specialized sensory structures such as bristles. They include the olfactory and mechanosensory bristles, as well as chordotonal organs (internally located stretch receptors that transduce auditory or proprioceptive stimuli). Each neuron in a type I organ bears a single sensory dendrite with a modified cilium. Type II sense organs are multidendritic neurons that lack cilia and specialized support cells. Their sensitivities are not known, but they also have been suggested to function as proprioceptors or mechanoreceptors (Jan and Jan, 1993).

Several mutants affecting sensory perception by type I sensilla have been isolated in *Drosophila* in screens for loss of mechanosensation (Kernan et al., 1994), audition (Eberl et al., 2000) or olfaction (Shiraiwa et al., 2000). Those that have been molecularly characterized include *nompC*, which encodes a member of the TRP channel superfamily (Walker et al., 2000), and *nompA*, a component of the dendritic cap that ensheaths the sensory cilium (Chung et al., 2001). In *nompA* mutants, defects in mechanosensory behavior and electrophysiology are associated with disconnection of dendritic caps from the

sensory cilia (Chung et al., 2001). Two other mutants specifically affecting chordotonal organs, *btv* and *tilB*, have axonemal defects illustrating the importance of axoneme integrity for chordotonal organ function (Eberl et al., 2000).

Structural components of cilia such as tubulins, tektins and axonemal dynein subunits have mostly been isolated from the single-celled alga *Chlamydomonas reinhardtii* and from sea urchin (Dutcher, 1995; Stephens, 1995) but are well highly conserved in other phyla. An intraflagellar transport (IFT) mechanism required for ciliary assembly is also widely conserved (Kozminski et al., 1993; Rosenbaum et al., 1999). Best characterized in *Chlamydomonas*, IFT is a rapid movement of particles along the axonemal microtubules of cilia and flagella. Although many individual proteins involved in cilium architecture and IFT are well described, factors that regulate and coordinate their expression are poorly understood. In *C. elegans*, one such factor is DAF-19, a member of the RFX family of transcription factors. Loss of function *daf-19* mutations result in the absence of cilia in sensory neurons, the only type of ciliated structures present in the nematode (Swoboda et al., 2000). DAF-19 regulates several genes required for normal sensory cilium formation, including components of the intraflagellar transport complex: *che-2*, *osm-1*, *osm-5* and *osm-6* (Haycraft et al., 2001; Qin et al., 2001; Swoboda et al., 2000).

RFX transcription factors are defined by a 76 amino acid DNA-binding domain with a characteristic wing-helix structure (Reith et al., 1990; Emery et al., 1996; Gajiwala et al., 2000). The yeasts *S. pombe* and *S. cerevisiae* each have a single RFX factor (Huang et al., 1998; Wu and McLeod, 1995), while five RFX proteins have been identified in mammals (Emery et al., 1996; Morotomi-Yano et al., 2002). Mammalian RFX5 is essential for the transcription of MHC class II genes in the immune response (for a review, see Reith and Mach, 2001), but little is known about the cellular functions of the other mammalian RFX proteins. Two Rfx genes can be identified in *Drosophila* (Durand et al., 2000) (FlyBase: http://flybase.harvard.edu:7081/). *Rfx* is homologous to *daf-19* and to mammalian *Rfx1*, *Rfx2* and *Rfx3*, whereas the second gene shares conserved motifs with *Rfx5*, the most divergent mammalian Rfx (A. L., unpublished). *Rfx* is expressed in the peripheral nervous system (PNS), in the brain and in the testis during *Drosophila* development (Vandaele et al., 2001).

We report the isolation and characterization of two *Rfx* alleles. We show that *Rfx* mutants have defects in chemosensory and mechanosensory behaviors and in mechanosensory electrophysiology. Remarkably, cellular and ultrastructural analysis demonstrate that loss of *Rfx* is associated with a severe disorganization of the cilia at the tip of the sensory neuron dendrites. These results identify *Rfx* as an essential regulator of sensory cilium morphogenesis in *Drosophila*.

MATERIALS AND METHODS

Drosophila genetics

P element mutagenesis

Males *A143.1F3/ry^{506}Sb^{1}P{ry^{+}=Δ2-3}99B* were crossed with *TM3, ry^{RK}Sb^{1}Ser^{1}/TM6B,Tb^{1}* and (*ry^{-}*) male progeny were selected. Southern blot hybridization and PCR were performed to determine breakpoints for each selected line. For EMS mutagenesis, isogenized *st^{1}e^{s}ca^{1}* males were fed with 25 mM EMS in 1% sucrose for 16 hours. EMS solution was then replaced by 1% sucrose for 72 hours and males were mated with *TM2,Ubx/TM6,SbTb* females. Single F_1 individuals were crossed to *Rfx^{49}/TM6,SbTb* and mutagenized chromosomes were selected based on lethal or un-coordination phenotypes over *Rfx^{49}*. Among 1000 individual crosses, a newly isolated allele *Rfx^{253}* did not complement *Rfx^{49}* for lethality.

Df(3R)hth (Rieckhof et al., 1997) chromosome was characterized by in situ hybridization performed on salivary glands from *Df(3R)hth/TM2* individuals. PCR analysis was performed to show that *S143702* (Deak et al., 1997) is a deficiency uncovering *jumu* and *Rfx* coding sequences. *S143702* homozygous embryos were isolated from *w; l(3)^{S143702}/TM3, P{w^{+}=GAL4-Kr}P{w^{+}=UAS-GFP.S65T},Sb^{1}* stock. DNA was extracted from pools of three embryos and PCR reactions were performed with the following primers: ATCTAACAGCAGCGCCACTT; CGACGGGACCACCTTATGTTATTTCATCATG; CGCCGGAATTCATCCTCTCG; TGTCATGACATCCTCCAGTG; CAAATTTGCCAATCATGTCG and ATTTCCCAAACGTCTGTTCG.

Complementation analysis shows *stich1^{D233}*, *stich1^{EP0359}* and *S143702* to be allelic to *jumu^{6439}*, a hypomorphic mutation of the *jumu* gene (Cheah et al., 2000; Strodicke et al., 2000). *S143702* is also allelic to *Rfx^{49}* in agreement with its molecular characterization. The P insertion line *l(3)06142* complements both *Df(3R)hth* and *S143702* leading to the conclusion that the lethal mutation on this chromosome maps outside the 85F-86C region, as previously hypothesized (Strodicke et al., 2000).

All stocks described were obtained from the Bloomington stock center, Indiana, with the exception of *Df(3R)hth* (a gift from R. Mann) and *sca$^{109-68}$* (a gift from J. M. Dura). *Drosophila* were grown on David's axenic food at 25°C (David, 1962).

Rfx rescue

The complete *Rfx* 3.9kb cDNA (Durand et al., 2000) was cloned in pUAST vector and subsequently injected in flies, as described (Spradling, 1986). Both GAL4 drivers, *P{GawB}elav^{C155}* and *P{GAL4}sca$^{109-68}$*, which express the protein in the entire nervous system (Luo et al., 1994) and in the peripheral nervous system (Guo et al., 1996), respectively, were used to rescue mutant phenotypes. Crosses were performed between stocks *ywP{GawB}elav^{C155}/FM7,w*; *sr^{1}Rfx^{253}e^{s}ca^{1}/TM6,HuTb* or *P{GAL4}sca$^{109-68}$*; *sr^{1}Rfx^{253}e^{s}ca^{1}/TM6,HuTb* and *w*; *P{w^{+}=UAS-Rfx}^{178}/CyO;Rfx^{49}/TM6,HuTb*. Rescued flies show a complete reversal of the uncoordinated phenotype and normal viability and reversal of the mutant phenotype was analyzed for the dendrite morphology by GFP labeling in adult legs and wings. Other phenotypes were not analyzed.

Sequencing and electromobility shift assay (EMSA)

Genomic DNA from *Rfx^{253}* flies was sequenced with primer sets covering all 11 *Rfx* exons by automatic sequencing using a MegaBACE sequencing facility. The *Rfx^{253}* mutation, a C to T transition at position 1899 of published sequence (EMBL Accession Number, AJ133103) changing a Ser to a Phe, was introduced into Rfx cDNA in pBluescript with Quickchange™ procedure (Stratagene). RFX^{253} or RFX protein was produced by in vitro transcription and translation. EMSA was performed as previously described (Durand et al., 2000).

Sensory perception assay

Olfactory and gustatory tests were performed essentially as described by Heimbeck et al. (Heimbeck et al., 1999). Larvae were selected on their *Tubby* (*Tb*) phenotype from appropriate crosses involving *Rfx^{-}/TM6BTb* heterozygotes. Each assays was performed with approximately 30 larvae. Amounts of olfactants placed on a small filter discs were 1 μl undiluted butanol (Merk 9630) or 2 μl of undiluted *n*-octyl-acetate (Sigma O-0504). We calculated a response

index (RI)=Ns-Nc/Ns+Nc. Ns represents the number of animals less than 30 mm from the odor source. Nc is the number of larvae found in an identical surface on the opposite (control) side. Positive RI indicate attraction. Negative RI indicate avoidance, and RI=0 indicates an indifferent behavior. For gustatory assays, petri dishes were divided in four quadrants filled with 1% agarose with a defined content of NaCl. The response index was calculated as RI=Ns-Nc/Ns+Nc, where Ns is the number of larvae on the high NaCl (1 M) quadrants and Nc is the number of larvae on the control (no NaCl) quadrants. Phototaxis assays were performed as described by Lilly and Carlson (Lilly and Carlson, 1990). Response index was calculated as RI=Nd-Nl/Nd+Nl, where Nl is the number of larvae in the light quadrants and Nd number of larvae in the dark quadrants. Significance of behavioral differences was assayed with nonparametric Mann-Whitney U tests (Mann and Whitney, 1947) and data are available upon request.

Electrophysiological recordings

Transepithelial mechanoreceptor potentials (TEP) and currents were recorded from single macrochaete bristles. Decapitated flies were mounted between 24 and 48 hours after eclosion as described (Walker et al., 2000). All recordings were performed on the posterior dorsocentral (pDC) and anterior scutellar (aSC) bristles on the dorsal thorax. Voltage and current signals were amplified (EPC7 amplifier; Heka Elektronik, Lambrecht, Germany) in current-clamp and voltage-clamp mode, respectively, and data were sampled at 5 kHz with an InstruNet 100 analog-to-digital converter and Superscope II software (GW Instruments, Somerville, MA). The reference ground was an Ag/AgCl wire inserted in the abdomen; zero potential was determined by placing the recording pipette in the thorax prior to recording from bristles. Bristles were mechanically stimulated with a 10 μm, 1.5 second ramp-and-hold displacement, generated by a piezoelectric actuator (PZS-100HS, Burleigh Instruments) on which the recording pipette was mounted. Mechanoreceptor potential (MRP) amplitude was calculated as the difference between the TEP just before the stimulus onset and the minimum TEP value reached during the stimulus. The transepithelial series resistance was calculated from the steady-state current resulting from a 10 mV step command applied to the recording pipette in voltage-clamp mode.

Sound-elicited potentials were recorded from the antennal nerve with tungsten electrodes inserted between the first and second antennal segments and in the head capsule as previously described (Eberl et al., 2000). Sound stimuli were generated and delivered as described (Eberl at al., 2000). They approximated the pulse phase of *Drosophila* courtship song and consisted of brief pulses of a 500 Hz carrier frequency repeated at 35 mseconds intervals.

Dendrite observation

For embryonic PNS observation, *Rfx⁻/TM2, P{ry⁺=ftz-lacZ}* stocks were used to differentiate mutant from heterozygous embryos based on their β-galactosidase staining [mouse anti-β-galactosidase (Promega; code Z3781)]. Mouse anti-22C10 (Zipursky et al., 1984) (kindly provided by S. Benzer) and affinity purified rabbit anti-HRP (Jackson Immunoresearch Laboratories; code 323-005-021) both at dilution 1:3000 were used. Antibodies were revealed with the Vectastain ABC kit for Nomarski observation or with Alexa Fluor® 546 goat anti-rabbit IgG and Alexa Fluor® 488 goat anti-mouse IgG (Molecular Probes) for confocal microscopy analysis.

To visualize GFP-expressing neurons, *wP{GawB}elav^{C155}P{w$^+$=UAS-mCD8:GFP}^{LL4}; Rfx⁻/TM6B* stocks were used. Wing campaniform sensilla were observed from adult wings fixed 15 minutes in 5% formaldehyde and observed under epifluorescence (Zeiss Axoplan). The femoral chordotonal groups were observed in dissected legs from 72-hour-old pupae, fixed for 15 minutes in 5% formaldehyde and imaged by confocal microscopy (Zeiss LSM510).

Electron microscopy

Antennae were dissected in PBS and immediately fixed in 2% glutaraldehyde, 0.5% paraformaldehyde and 0.1 M Na-cacodylate (pH 7.4) for 48 hours. After extensive washing in sodium cacodylate 0.15 M (pH 7.4), antennae were stained in 1% OsO_4 for 4 hours, and dehydrated through ethanol series and propylene oxide. Antennae were embedded in Spurr medium (Fluka). Ultrafine sections were cut on a Leica ultramicrotome. Sectioned materials were contrasted in Leica ultrastainer in alcoholic uranyl acetate and lead citrate.

RESULTS

Generating *Rfx* mutations

Rfx is located on the third chromosome at 86A1-2 and is flanked by two genes transcribed on the opposite strand: *jumu* (also described as *Dom)* and *CG17100* (Fig. 1A). This latter was previously suggested to be affected in *stich1* mutants (Prokopenko et al., 2000). We first investigated available deficiencies in the 86A-B domain that would uncover *Rfx*. We show that *Df(3R)hth* uncovers *Rfx*, as visualized by polytene chromosome in situ hybridization with a *Rfx* probe (Fig. 1B). Moreover, no trace of RFX protein is detected in *Df(3R)hth* homozygous embryo tissues by immunostaining (data not shown). All together with complementation results (Table 1) these data indicate that *Df(3R)hth* is a deficiency uncovering the entire 85F-86C region.

A P-element inserted 5′ of *Rfx* (*A143.1F3*) was mobilized to generate more aberrations affecting the *Rfx* locus (Fig. 1A). Several chromosomes were selected by molecular screening, including *Rfx^{49}*, a small deficiency uncovering the 5′ end of *Rfx* (Fig. 1A). Molecular characterization of *Rfx^{49}* breakpoints revealed that the deletion does not uncover the adjacent *jumu* gene. Indeed, *Rfx^{49}* complements the lethal phenotype of all *jumu* lethal alleles tested (Table 1). Moreover, no RFX

Table 1. Complementation analysis of the lethal phenotype of mutants in the 86A-B cytological region

	A143.1F3	*jumu^{6142}*	*jumu^{6439}*	*stich1^{EP0359}*	*stich1^{D233}*	*S143702*	*Rfx^{49}*	*Rfx^{253}*	*Df(3R)hth*
A143.1F3	PL	V	V	V	V	V	V	V	V
jumu^{6142}		L	V	ND	V	V	V	V	V
jumu^{6439}			L	L	L	L	V	V	L
stich1^{EP0359}				L	L	L	V	V	L
stich1^{D233}					L	L	V	V	L
S143702						L	L	L	L
Rfx^{49}							L	L	L
Rfx^{253}								L	L
Df(3R)hth									L

L, lethal, no viable expected adults in standard rearing conditions; PL, pseudo-lethal, less then 10% of viable expected progeny; V, viable; ND, not done.

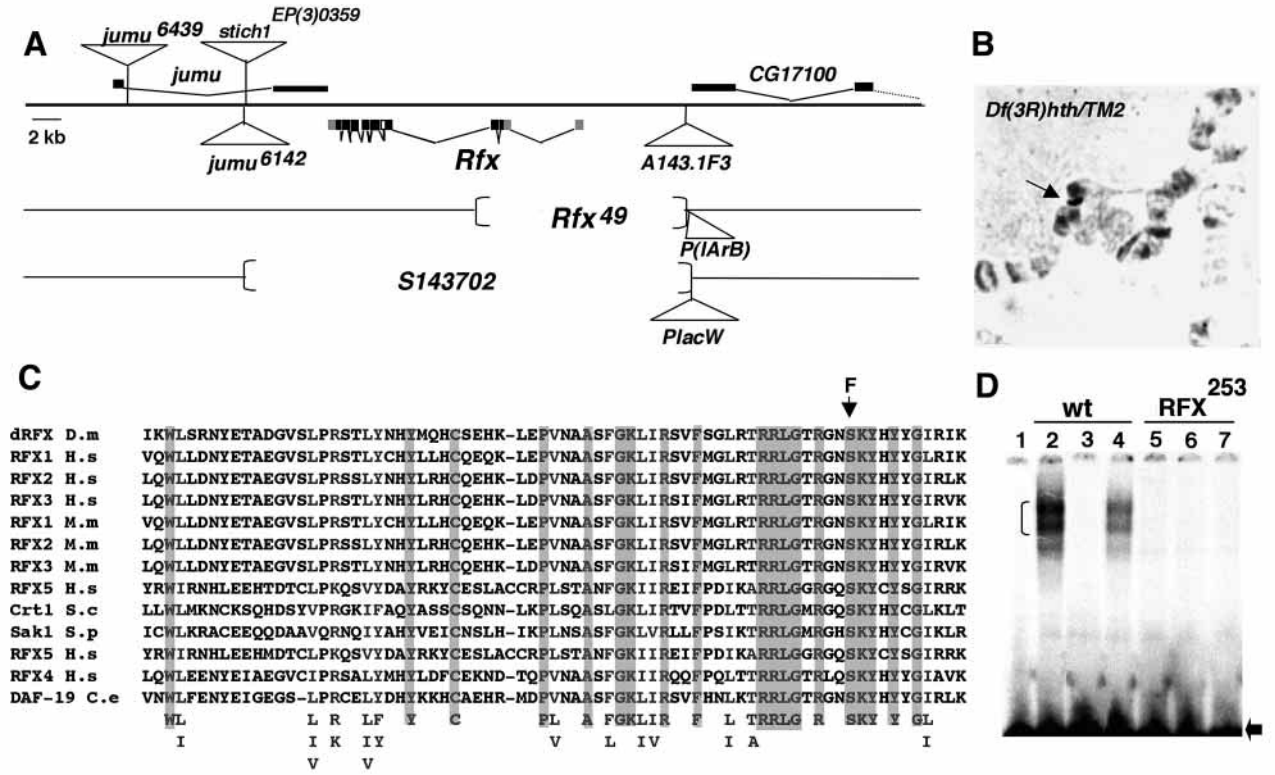

Fig. 1. *Rfx* locus and genetic elements. (A) The organization of the *Rfx* genomic region on chromosome III, centromere to the left. The four P-element insertions and the two deficiencies described in this study are reported. Two elements (*jumu*^{6142}, *jumu*^{6439}) are located in the *jumu* gene. The element of the *A143.1F3* line is inserted 5′ of *Rfx* and 5′ of the *CG17100* gene transcription start site. The S143702 P element is inserted in the *jumu* gene. The insertion event has generated a deficiency uncovering *Rfx* and *jumu*-coding regions. The remaining PlacW element is situated at the deficiency breakpoints. *Rfx*^{49} is a small deficiency uncovering the first three exons of *Rfx* created by *A143.1F3* mobilization. 4 kb of the *A143.1F3* P(lArB) element remain in *Rfx*^{49} at the deficiency breakpoints. (B) *Rfx* in situ hybridization of *Df(3R)hth/TM2* salivary gland polytene chromosomes. *Rfx* hybridization (arrow) allows the visualization of the loop on the third chromosome because of a complete deficiency of the 85F to 86C regions on chromosome *Df(3R)hth*. (C) Alignment of RFX DNA-binding domain from different species. *Rfx*^{253} corresponds to a point mutation changing an absolutely conserved serine to a phenylalanine within the DNA-binding domain. Species abbreviations: *H.s., Homo sapiens; M.m., Mus musculus; D.m., Drosophila melanogaster; C.e., Caenorhabditis elegans; S.c., Saccharomyces cerevisiae; S.p., Schizosaccharomyces pombe*. (D) Electromobility shift assay with in vitro translated wild-type RFX or RFX^{253}, and an X box-labeled oligonucleotide. Lane 1, no protein; lanes 2-4, RFX; lanes 5-7, RFX^{253}; lanes 2,5, no competitor; lanes 3,6, X box oligonucleotide as competitor; lanes 4,7, mutated X box oligonucleotide as competitor; RFX^{253} is not able to bind an X box oligonucleotide. The arrowhead indicates the free probe. The bracket indicates RFX-DNA complex.

immunostaining was found in the peripheral nervous system (PNS) of *Rfx*^{49} mutant embryos (data not shown) compared with wild-type embryos (Vandaele et al., 2001).

Complementation analysis with *Rfx*^{49} and *Df(3R)hth* chromosomes identifies two complementation groups in the 86A1-2 region that we define as *jumu* and *Rfx* (Table 1). Our analysis shows that all *stich1* alleles fail to complement *jumu* loss of function alleles. We also showed by PCR analysis that *S143702* is actually a deficiency uncovering both *jumu* and *Rfx* loci (data not shown, see Materials and Methods). All together these results imply that *stich1* mutations affect the *jumu* gene but not CG17100.

The more distal breakpoint of *Rfx*^{49}maps 100 bp upstream of the 5′ end of CG17100. It is therefore theoretically possible that *Rfx*^{49} also affects this gene. We thus undertook an EMS non-complementation screen to isolate other *Rfx* alleles (see Materials and Methods) and isolated the *Rfx*^{253} chromosome, which defines the same complementation group as *Rfx*^{49} (Table 1). Sequencing analysis revealed a mutation causing an amino acid substitution, S^{435}F, in the DNA-binding domain (Fig. 1C). Serine at position 65 of the DBD is replaced by a phenylalanine. Remarkably, the mutated serine is absolutely conserved in all RFX proteins described from yeast to mammals (Fig. 1C) and, in a crystallographic structure of the mammalian RFX1 DBD, is located in the ‘wing’ loop that mediates most DNA contacts (Gajiwala et al., 2000). We confirmed by electromobility shift assay that *Rfx*^{253} is no longer able to bind its target sequence (Fig. 1D). Thus, based on its lack of DNA binding, *Rfx*^{253} represents a hypomorphic or null allele of *Rfx*.

Rfx larvae are insensitive to chemical or odorant stimuli

Under standard rearing conditions, most *Rfx*^{49} and *Rfx*^{253} homozygotes die as larvae. Mutant pupae could not be observed on the walls of the culture vials, regardless of allelic combination. However, in uncrowded conditions, a small proportion of homozygous pupae were detected on vials, indicating that a few larvae can pupate. Approximately 15% of first instar larvae give rise to pupae. Mutant larvae lag their

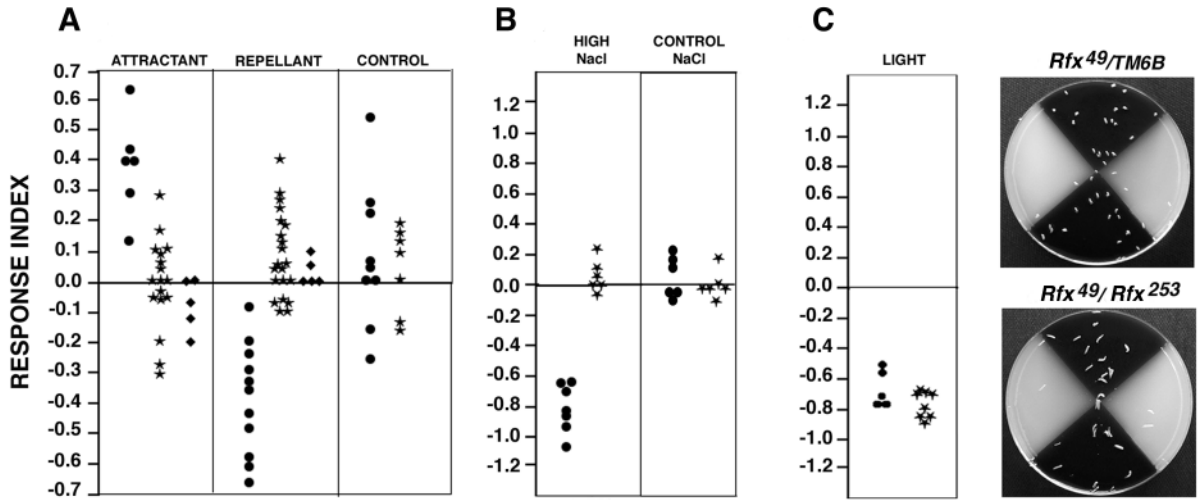

Fig. 2. Sensory behaviors of *Rfx* mutants. Three different assays were performed and the corresponding data are plotted. Each point is the response index obtained with ~30 larvae per individual test. Dots represent $Rfx^{253}/TM6B,Tb$ larvae; stars indicate Rfx^{49}/Rfx^{253} larvae; diamonds indicate Rfx^{49}/Rfx^{49} larvae. (A) Data for olfactory assays to attractive (butanol), repulsive (*n*-octyl-acetate) or non odorant (NaCl) control substances. (B) Data for chemosensory assays to high NaCl concentrations or control NaCl concentrations. (C) The result of a typical phototaxy experiment with $Rfx^{49}/TM6B$ control larvae on top and Rfx^{49}/Rfx^{253} mutant larvae on the bottom. The plot shows the quantification of phototaxis assay data.

heterologous siblings by more than 3 days in development to pupae. Close observation of larvae show a peculiar foraging behavior with weak food digging efficiency. This could result from an altered peripheral sensitivity, a hypothesis that was suggested by the fact that *Rfx* is expressed in sensory neurons during embryogenesis (Vandaele et al., 2000). We thus decided to investigate the gustatory and olfactory-driven behavior of mutant larvae.

An olfactory test was performed using two pure odors (butanol and *n*-octyl-acetate) that induce characteristic attractive and repulsive responses (reviewed in Cobb, 1999). Whereas control larvae responded efficiently, mutant larvae showed no sensitivity to either odor (Fig. 2A). We also assayed repulsion by high NaCl concentrations: while control larvae are repulsed by concentrated salt, mutant larvae do not avoid this medium (Fig. 2B), showing that *Rfx* mutant larvae are defective in gustatory chemotaxis as well. To demonstrate that these responses are not due to a defect in the larval motility, we tested phototaxis behavior (Fig. 2C). This is based on our finding that *Rfx* is not expressed in the Bolwig organs, the larval visual system (Vandaele et al., 2001). *Rfx* mutant larvae should therefore not be affected in visual perception. This was clearly demonstrated by the phototaxis behavioral assay as shown in Fig. 2C. The phototaxis behaviors of *Rfx* mutant and control larvae were found to be identical, demonstrating that *Rfx* mutants are not affected in their capacity to move. These data lead to the conclusion that *Rfx* is necessary for olfactory and gustatory perception in *Drosophila* larvae.

Rfx adults have an uncoordinated phenotype and do not transduce mechanosensory stimuli

Emerging adults are not able to walk and fly and thus stick to the medium and cannot be retrieved in culture vials. In order to recover adult mutants, third instar larvae and pupae were selected and raised until hatching on wet filter paper. The 15 to 30% of Rfx^{49}/Rfx^{253} or $S143702/Rfx^{253}$ adults that emerge from pupae, all present a characteristic uncoordinated phenotype. Mutant flies cannot stand or walk: legs are crossed and wings are held up. However, mutants do react to light stimulation by moving legs and wings in an effort to right themselves and walk, but uncoordination limits their movement to a few steps or a flip from one side to another. This transient activity indicates that general neuromuscular excitability is retained. To ascertain that *Rfx* is responsible for the observed phenotype, an *Rfx* cDNA was expressed in all neurons in Rfx^{49}/Rfx^{253} mutants. We found that the transgene expression indeed completely rescued the Rfx^{49}/Rfx^{253} uncoordinated and low viability phenotypes.

The uncoordination of *Rfx* mutant flies is similar to the phenotype of mutants with defects in mechanosensory transduction (Kernan et al., 1994). Type I external mechanosensory bristles include three support cells and one neuron (Fig. 3A). The innermost support cell (sheath cell) forms a tubular extension around the sensory process and produces an extracellular dendritic cap that covers the cilium tip (Keil, 1997). The two outer support cells (shaft and socket cells) construct the cuticular bristle socket and shaft and in mature organ generate the receptor lymph. To test if *Rfx* mutants also have defects in mechanosensory bristle electrophysiology, transepithelial potentials (TEPs) and currents were recorded from macrochaete bristles (Fig. 3A). Unstimulated wild-type bristles have a positive TEP, due to electrogenic K^+ transport by sensory support cells into the restricted apical extracellular space. This creates the electrical driving force for a receptor current that is triggered by bristle deflection: current flows from the apical extracellular space into the sensory neuron, reducing the TEP and depolarizing the neuron so that it fires a series of action potentials (Thurm and Kuppers, 1980) (Fig. 3B,C). The response adapts to a sustained deflection.

The average resting TEP in *Rfx* mutants (12±9 mV) is significantly lower than in their heterozygous sibs (61±4 mV), although the mutant and control distributions overlapped (Fig. 3C,E). More strikingly, no mechanically elicited changes in TEP were detected in any *Rfx* mutant bristle, even in bristles

with TEP in the normal range (Fig. 3D). Holding the TEP constant while stimulating the bristle enables a mechanoreceptor current to be recorded (Walker et al., 2000) (Fig. 3F,G). No receptor currents were elicited by mechanical stimulation in *Rfx* mutants, even when the TEP was clamped at a large positive value (+100 mV; data not shown). Finally, no action potentials were observed in mutant neurons. Thus, the adult uncoordination phenotype probably reflects a failure of bristle mechanotransduction. Maintenance of the TEP requires both active ion transport by sensory support cells, and high cuticular and transepithelial resistance. The resistance at *Rfx* mutant bristles was found to be, on average, one-third that at control bristles (Fig. 3H), suggesting some reduction in the integrity of the intercellular junctions connecting the neuron and the surrounding support cells.

Most mechanosensory mutations affect chordotonal organs as well as bristles (Eberl et al., 2000). Chordotonal organs are type I stretch receptors that transduce proprioceptive and auditory stimuli. To test chordotonal organ operation, extracellular sound-elicited potentials were recorded from the antennal nerve projecting from the auditory chordotonal organs (Johnston's organ, Fig. 3I) in wild-type and mutant antennae. Johnston's organ comprises over 100 individual sensory units or scolopidia located in the second antennal segment, which normally respond when distal antennal segments are vibrated by near-field sound (Eberl et al., 2000). A series of sound pulses elicited a corresponding response from $Rfx^{49}/TM6B$ heterozygotes, but Rfx^{49}/Rfx^{253} mutants showed no response to stimuli of the same or greater amplitude, indicating a complete loss of auditory chordotonal organ function (Fig. 3J).

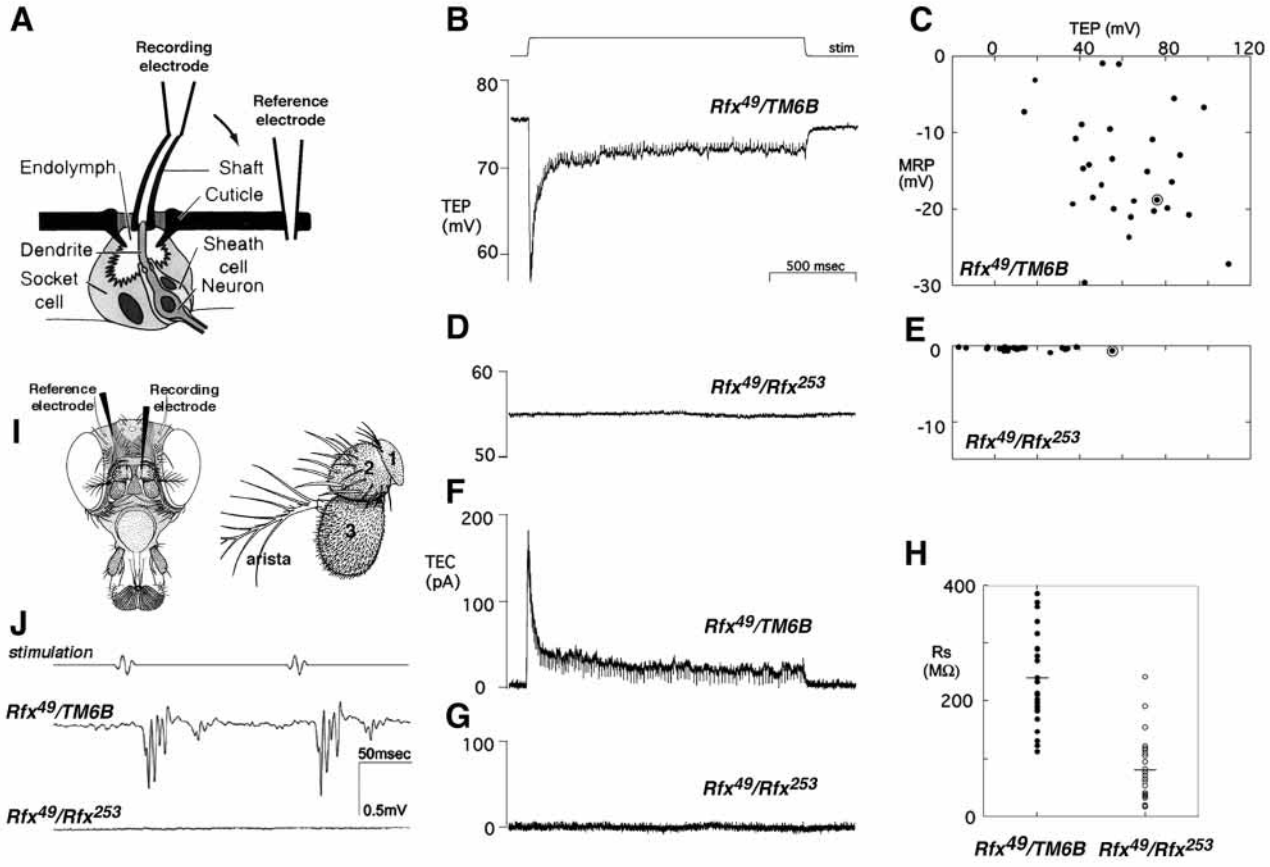

Fig. 3. Electrophysiological recordings from adult *Drosophila* external mechanosensory organs. (A) Diagram of a *Drosophila* mechanoreceptor bristle, adapted from Walker et al. (Walker et al., 2000). The bristle sensory organ is composed of a hollow hair shaft and three cells: the socket cell, the sheath cell and a ciliated mechanosensory neuron. The recording configuration consisted of two electrodes: a reference electrode placed in the abdomen of the fly and a recording/stimulation electrode slipped over the cut end of a bristle. (B-E) Mechanically elicited changes in transepithelial potential (TEP) recorded from single macrochaete bristles in $Rfx^{49}/TM6B$ (B,C) and Rfx^{253}/Rfx^{49} (D,E) flies. (B,D) Representative single traces; the 10 μm stimulating displacement is shown in B. In C,E, the maximum amplitude of the mechanoreceptor potential (MRP) in each bristle is plotted against its resting TEP. Circled points correspond to the traces shown in B,D. (F,G) Transepithelial currents (TEC) recorded from the same bristles, with apical holding potentials of +76 mV and +55 mV, respectively. The stimulus displacement is as in B. No mechanically elicited currents were observed in *Rfx* mutant flies. (H) Transepithelial resistance in $Rfx^{49}/TM6B$ (n=27, mean=243±16 MΩ) and *Rfx* mutant (n=24; mean=80±12 MΩ) bristles. Points are values for individual bristles; lines indicate the mean resistance. Transepithelial resistance is significantly reduced ($P<10^{-9}$) in *Rfx* mutants. (I) Diagrams of a *Drosophila* head showing the position of the electrodes used to record sound-elicited potentials, and of an antenna indicating the different segments. The Johnston's organ is situated in the second antennal segment (2). Chordotonal organs attached to the joint between the second and third segments are stimulated by vibration of the arista and third segment (3). (J) Sound-elicited potentials recorded from $Rfx^{49}/TM6B$ control or Rfx^{253}/Rfx^{49} mutant antennae in response to pulse sound stimulation. Each trace is an average of the responses to ten consecutive stimulus trains. No sound-elicited potentials were detected in mutant antennae.

Taken together, the broad spectrum of behavioral and electrophysiological defects suggested that all type I organs are affected in *Rfx* mutants. This idea was further pursued by light and electron microscopy.

Type I sensory dendrite morphogenesis is affected in *Rfx* mutants

To examine the morphology of sensory neurons in *Rfx* mutants, we used a series of molecular markers for the peripheral nervous system (PNS). With the 22C10 antibody, which stains a microtubule-associated protein in all sensory neurons, we observed no differences in number and position of sensory neurons between mutant and wild-type embryos (Fig. 4A,B). By contrast, the anti-HRP antibody, which stains all neuron surfaces in wild-type embryos, revealed a very weak staining of the PNS in the mutant embryos regardless of the *Rfx* allelic combination used (Fig. 4C,D). An identical weak anti-HRP staining of sensory neurons was also reported for *S143702* embryos (Prokopenko et al., 2000) but not for the other *stich1* mutants, confirming that this phenotype is specifically due to loss of *Rfx* function.

Anti-HRP staining in mutant embryos was, however, strong enough to visualize a specific dendrite defect, particularly visible in the lateral chordotonal organ clusters (lch5). Indeed, this array of chordotonal organs is disorganized in *Rfx* embryos. Most dendrites are shorter, and vary in length within a cluster (Fig. 4E-H). The cilia present in wild type (Fig. 4C,E) or control (Fig. 4G) embryos were always either shorter or missing in *Rfx* mutants (Fig. 4F,H).

To visualize neuronal dendrites in more detail, we engineered mutant flies expressing a membrane-localized GFP in all neurons. We focused on two types of adult sensory organs: campaniform sensilla of the wing and chordotonal organs of the femur.

Campaniform sensilla of the wing are composed of a single neuron and three accessory cells. The neuronal cell body and the dendrite are situated in the same focal plane and are thus easily visible when marked with GFP. The cilium at the tip of the dendrite is located exactly under the dome-shaped sensilla in wild-type (not shown) or in rescued wings (Fig. 5A-B). In *Rfx* mutant wings, the dendrite does not reach the dome and the cilium is either absent, or shorter (Fig. 5C-E).

In the femoral chordotonal organ, each scolopidium is innervated by two ciliated neurons. Instead of external cuticular structures, a rigid scolopale structure encloses the ciliary outer segments. By confocal microscopy analysis of GFP distribution, three ciliary regions can be distinguished, which correlate with an ultrastuctural organization previously described by transmission electron microscopy (Uga and Kuwabara, 1965). These are: the axoneme, the ciliary dilation and the tubular body enclosing the tubular bundle (a dense array of microtubules). These subregions are clearly distinguished in control or rescued *Rfx* mutant flies (Fig. 5F-I). By contrast, the cilium is always shorter (Fig. 5J-L) and even absent (Fig. 5K,L) in mutant flies. When present, no clear cilium subregions can be distinguished indicating that its architecture is very disorganized. Moreover the inner dendritic segment appears swollen (Fig. 5J-L, arrowheads). These defects were specifically rescued when the *Rfx* cDNA was expressed in all neurons thus demonstrating that *Rfx* expression in the neuron is necessary for differentiation of the ciliated sensory ending in adult sense organs.

No organized ciliated structures can be observed in type I neurons of *Rfx* mutants

Investigation of the ultrastructure of sensitive neurons was carried out on the Johnston's organ in the second antennal

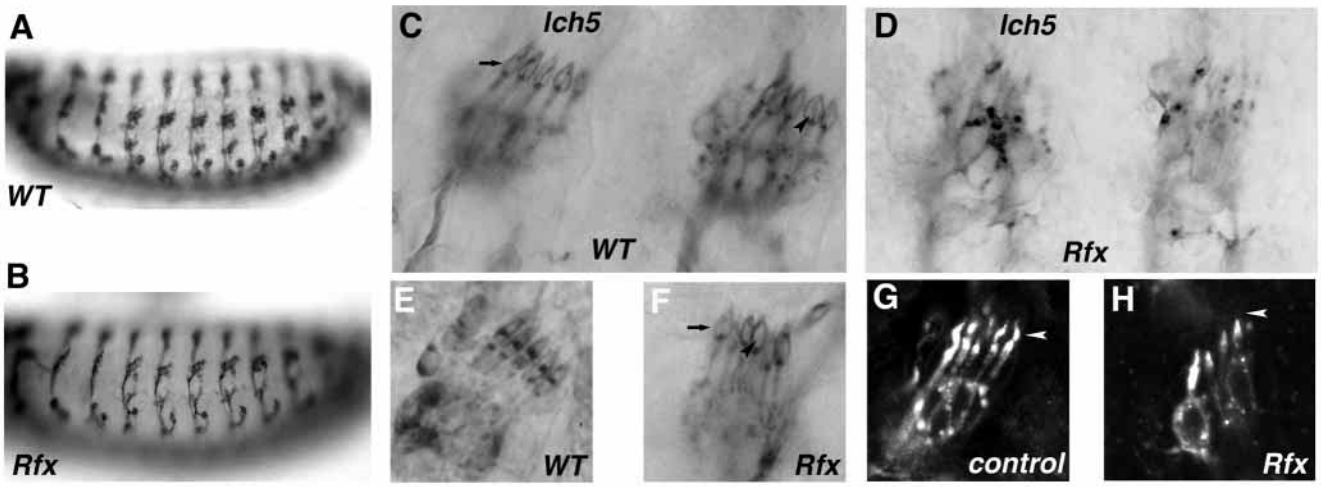

Fig. 4. Type I sensory neuron defects in *Rfx* mutant embryos. Embryonic peripheral nervous system was observed by immunostaining in wild-type and *Rfx* mutant embryos. Nomarski observation of 22C10 staining on wild-type (A) or Rfx^{49} mutant embryos (B). No differences in the number and position of PNS neurons are observed. (C-H) Anti-HRP staining of wild-type (C,E), control $Rfx^{253}/TM6B$ (G) or Rfx^{49} mutant (D,F,H) lateral chordotonal organs (lch5). Staining is revealed with a peroxidase-coupled secondary antibody (C-F) and with a fluorescent secondary antibody (G-H). In mutant embryos, staining is strongly affected and neuron groups appear disorganized (D). When staining is strong enough to visualize dendrites in mutant embryos, cilia (arrowhead) are often absent (F) when compared with wild-type embryos (C,E). Note the labeled dendritic cap (arrow) enclosing the cilium also present in wild-type (C) or mutant embryos (F). (G,H) Fluorescent labeling allows accurate visualization of the terminal dendritic structures caused by a faint staining of the dendritic cap. In *Rfx* mutant embryos (H) the cilium (arrowhead) is always shorter or absent compared with control embryos (G).

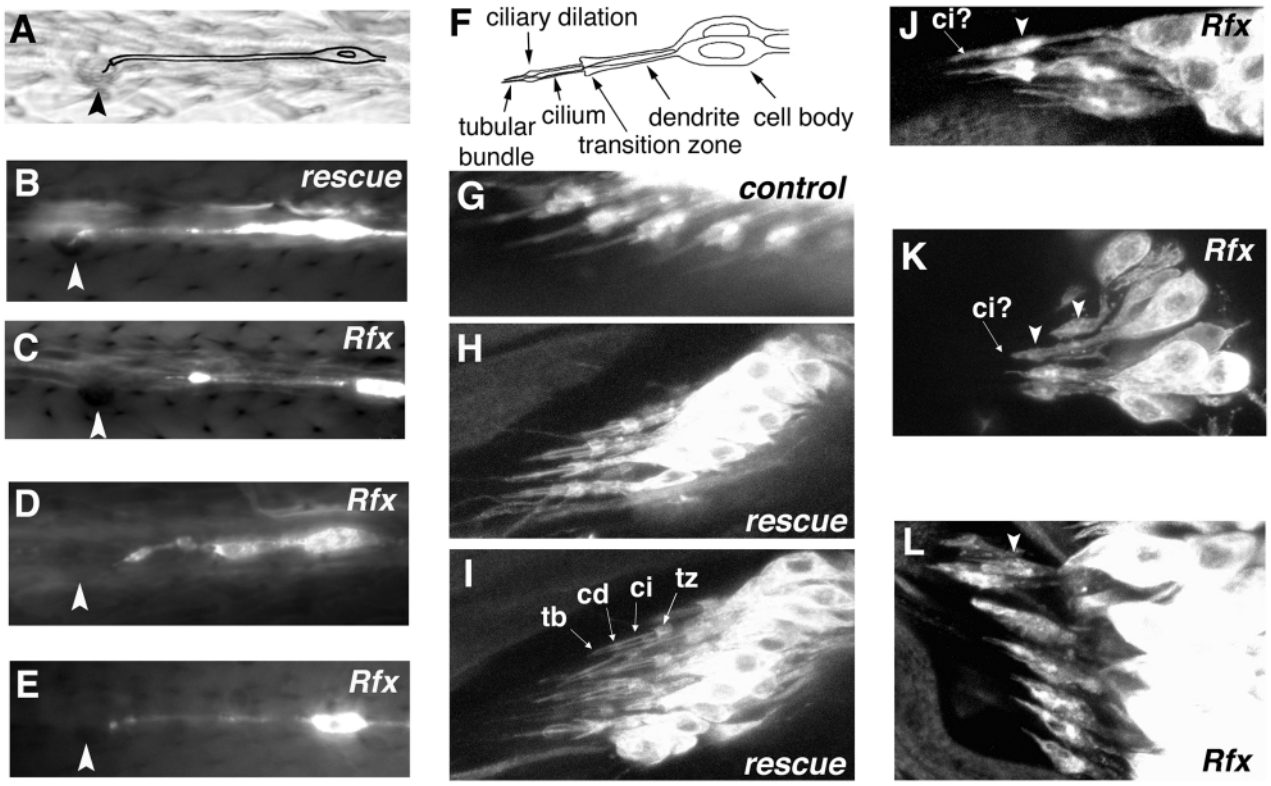

Fig. 5. Dendrite defects in late pupal or adult type I sensory neurons. All neurons are labeled with mCD8-GFP. (A) A scheme representing the neuron innervation of a campaniform sensillum of the adult wing vein. Arrowhead indicates the dome-shaped structure of the sensillum. (B-E) Dendrite observation in adult wing campaniform sensilla. Arrowheads indicate the position of the dome shaped sensilla. In control (not shown) or rescued Rfx^{253}/Rfx^{49} mutant wings (B), the cilium is located just under the dome-shaped sensory structure produced by the accessory cell. In all Rfx^{253}/Rfx^{49} mutant wings (C-E), the dendrite is never situated under the dome-shaped sensilla and sometimes ends well before the sensillum (C). In most cases, the cilium is either shorter or absent (D,E). (F) A schematic representing the two neurons innervating a chordotonal organ of the femur as observed in G-L. In $Rfx^{253}/TM6B$ (G) or rescued Rfx^{253}/Rfx^{49} mutant pupae (H,I), the three subregions of the cilium are clearly visible. tb, tubular bundle; cd, ciliary dilation; ci, cilium; tz, transition zone. In mutant legs (J,L), the cilium is either absent or shorter (arrows) and distinct subregions cannot be distinguished. The dendritic transition zone appears swollen (arrowheads). (J) $Rfx^{49}/S143702$; (K) Rfx^{49}/Rfx^{253}; (L) $Rfx^{253}/S143702$.

segment. Each scolopidium of the Johnston's organ includes two neurons, a scolopale cell and an elongated conical dendritic cap that encloses the distal tips of the two cilia (Fig. 6A). The tips of a pair of cilia are attached via an extracellular cap to a distal attachment cell (cap cell), and their bases are anchored within the neurons by a long axial filament that extends through the neuronal dendrites and cell bodies. Cross-sections performed at different proximodistal positions reveal the three different typical ultrastructural subregions of chordotonal cilia (Fig. 6A). The sensory cilium is composed of 9+0 microtubule doublets. The ciliary dilation contains a paracrystalline inclusion and the tubular body is composed of microtubule arrays that are not assembled in a stereotyped fashion as in the cilium. The two cilia are surrounded by electron dense structures (scolopale rods) produced by the scolopale cell. The cilium at the tip of the dendrite contacts an extracellular matrix (dendritic cap).

Examination of sectioned antennae of *Rfx* mutants by light microscopy showed no gross defects in Johnston's organ, but the ultrastructure of individual scolopidia was profoundly altered. Sections of several scolopidia at different proximodistal positions (Fig. 6B,C) clearly show the 9+0 axonemal structure in wild-type antennae, but no axoneme profiles were found in serial sections of Rfx^{253}/Rfx^{49} antennae (compare Fig. 6B,D with 6C,E). In longitudinal sections the anchoring axial filament could be clearly observed in wild type (Fig. 6I), but not in mutant scolopidia (Fig. 6J). Its absence indicates that *Rfx* mutant defects extend beyond the cilium proper and affect associated structures in the neuron. In addition, a non-neuronal defect was noted: the electron dense scolopale rods enclosing the cilium are not as regularly arrayed as in wild-type flies (Fig. 6B,C). By contrast, the dendritic cap, also produced by the scolopale cell appears equally well organized in wild type and in *Rfx* mutants (Fig. 6F-H). These results demonstrate that *Rfx* is necessary for proper cilium assembly in chordotonal organs.

DISCUSSION

We have isolated two *Rfx* mutations that define a novel pseudo-lethal complementation group. One of these mutations, Rfx^{253} alters an absolutely conserved serine in the DNA-binding domain. This mutation is the first one affecting the RFX DNA-binding domain, thus confirming its importance for the biological function of RFX transcription factors. It supports

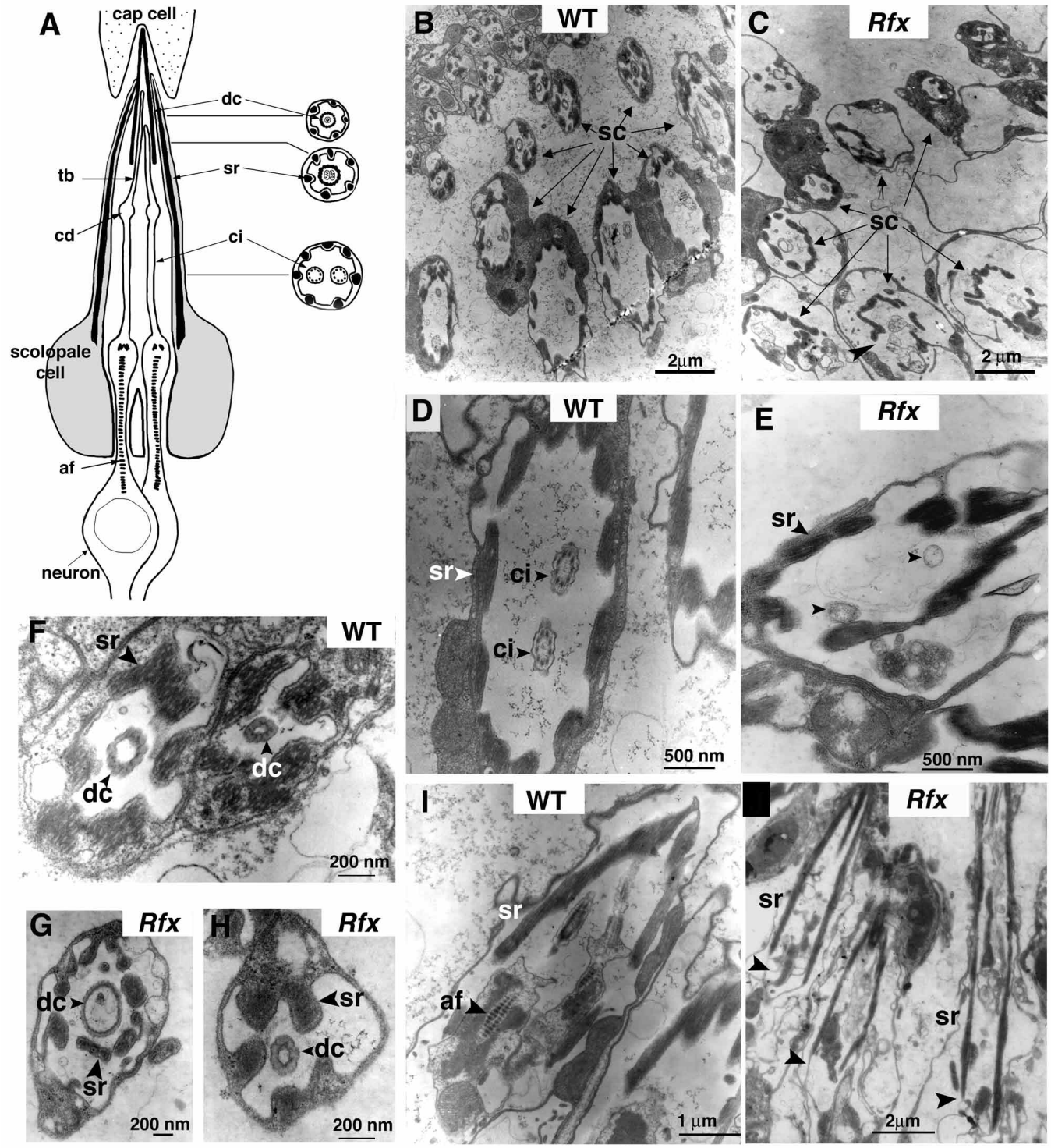

Fig. 6. Ciliary defects in *Rfx* mutants. (A) An antennal scolopidium of the Johnston's organ in longitudinal and cross-sections. tb, tubular bundle; cd, ciliary dilation; af, axial filament; dc, dendritic cap; sr, scolopale rods; ci, cilium. (B-J) Transmission electron micrographs of scolopidia of the Johnston's organ of wild-type and *Rfx* mutant adults. Cross-sections of wild-type (B,D,F) and Rfx^{253}/Rfx^{49} scolopidia (C,E,G,H). Longitudinal sections of wild-type (I) or Rfx^{253}/Rfx^{49} scolopidia (J). In B,C, scolopidia (sc, arrows) are sectioned at different levels from distal (up) to proximal (down). (B) Cilia are observed on proximal sections in wild-type antenna. (C) Scolopidia are less well organized and no typical cilia are observed in the *Rfx* mutant antenna, the arrowhead indicates a noticeably disorganized scolopidium. (D) Enlargement of a typical proximal section of a wild-type scolopidium presents the nine microtubule doublets (ci, arrowhead). (E) Enlargement of a proximal section of a *Rfx* mutant scolopidium shows that no microtubule doublet is present (arrowhead). (F-H) Enlargement of distal scolopidia sections. No differences are observed between wild-type (F) and Rfx^{49}/Rfx^{253} mutant (G,H) dendritic cap structures. (I,J) Longitudinal sections through scolopidia. (I) The axial filament clearly appears in the control dendrite process. (J) No typical axial filament is observed at the expected position (arrowheads) in longitudinal section of three *Rfx* mutant scolopidia.

predictions from crystallographic studies showing that this serine residue contacts DNA (Gajiwala et al., 2000).

We demonstrate that *Rfx* function in ciliated sensory neurons is essential for the proper signaling in type I sensory organs. *Rfx* mutant larvae have severe chemosensory and olfactory defects. These sensory defects could explain their peculiar, potentially insufficient foraging and feeding behavior, and could thus be responsible for major developmental delays, leading to lethality at significant frequencies. Moreover, consistent with their adult uncoordinated phenotype, *Rfx* mutant bristles show clear electrophysiological defects: they are completely unable to generate mechanoreceptor potentials or currents. The reductions in resting transepithelial potentials and transepithelial resistance are not sufficient to explain the complete loss of transduction, as mutants with TEPs in the normal range still showed no receptor current, and receptor currents could not be restored by voltage clamping the TEP at wild-type levels. Although recordings were limited to mechanosensory macrochaete bristles, the combination of mechanosensory and chemosensory behavioral phenotypes suggests a global defect in type I sense organ function, consistent with the pattern of *Rfx* expression.

Remarkably, we show that sensory defects are correlated with abnormal morphogenesis of the dendrite, which affects primarily the organization of its ciliated sensory endings. Indeed *Rfx* mutants show sensory dendrites that have severe cilium defects in femoral chordotonal organs as well as wing campaniform sensilla. This probably reflects a general defect in cilium assembly, as both the proximal and the distal parts of the organelle are disorganized: that is both rootlet apparatus and axonemal structures are absent from scolopidia in *Rfx* mutant antennae as observed by electron microscopy. All together, our observations show that the dendrite cilium is required for signal transduction in these neurons.

Mutant sensory defects are not restricted to the cilium

The observed mutant sensory defects are probably not restricted to only cilium disorganization. Indeed, electron microscopy reveals that the scolopale cell of chordotonal organs is also modified in the mutant antennae: the scolopale rods and membranes are disorganized compared with wild type. A similar effect on the sheath cell (the homolog of the scolopale cell in bristle organs) and other supporting cells could underlie the reduced epithelial resistance and TEP observed in *Rfx* mutant bristles. *Rfx* is expressed as early as the first neural precursor and is maintained throughout successive asymmetric division in the type I neuron lineage. *Rfx* is transiently expressed in the accessory scolopale cell (Vandaele et al., 2001). It could thus be necessary for proper accessory cell differentiation and in particular for cell junction formation between these cells.

Another observation suggesting that mutant defects are probably not exclusively restricted to the cilium is the reduced anti-HRP staining in mutant embryos. Anti-HRP has been shown to bind to neuronal membranes (Jan and Jan, 1982). It is known to recognize an epitope of carbohydrate origin, an α1,3-fucosylated, N-linked glycan (Fabini et al., 2001; Snow et al., 1987) associated with proteins such as Nervana-2, an Na^+K^+ ATPase expressed in all neurons, and with cell adhesion molecules, Fasciclin I and II, neurotactin and neuroglian (Desai et al., 1994; Sun and Salvaterra, 1995; Wang et al., 1994). In *Rfx* mutants, either the expression of these proteins is downregulated or the relevant post-translational modification does not operate efficiently. Interestingly, a reduction in anti-HRP staining is seen in both type I and non-ciliated type II PNS neurons, even though no morphological defects of type II neurons are observed by anti-HRP labeling (data not shown). Type I and type II neurons arise from common precursors (Orgogozo et al., 2001) expressing *Rfx*, but the latter lose *Rfx* expression upon differentiation and only type I neuron lineage express *Rfx* throughout embryonic development (Vandaele et al., 2001). Anti-HRP staining phenotype may suggest that all PNS neurons do not reach full terminal differentiation in *Rfx* mutant. *Rfx* transient expression in type II precursors could also be necessary for their differentiation. The anti-HRP staining phenotype could thus reflect a more general function for *Rfx* during neuronal differentiation.

Cilium defects are associated with dendrite morphogenesis defects such as incorrect positioning in the wing, swollen shape in the femur and the wing. We do not know if the cilium defect is responsible for these abnormal dendrite differentiations. The swollen dendrite could be a consequence of a defect in outward transport of intraflagellar transport, resulting in an accumulation of unassembled cilium components. The cilium defect could be responsible for incorrect dendrite positioning by disrupting close interactions between the cilium and structures of the sheath and the hair cell. Interestingly, the dendritic cap in the Johnston's chordotonal organ is not affected by cilium defects, which suggests that its production by the scolopale cell does not depend on the cilium. Analyzing *Rfx* regulatory pathways with the mutants we produced will allow to clarify these questions.

Rfx and ciliogenesis

Cilia are assembled through a process called intraflagellar transport (IFT) (Rosenbaum et al., 1999) first described in the unicellular green alga *Chlamydomonas* and highly conserved throughout evolution. *osm-1*, *osm5* and *osm-6*, which encode proteins involved in IFT are under the control of *daf-19*, the sole *RFX* gene in *C. elegans* (Swoboda et al., 2000; Haycraft et al., 2001; Qin et al., 2001). *osm-1* and *osm-6* encode homologous proteins to *Chlamydomonas* IFT polypeptides p172 and p52 (Cole et al., 1998; Collet et al., 1998). *osm-5* encodes a protein involved in cilium assembly and is homologous to *Chlamydomonas* IFT88 protein and to a mouse protein called Tg737/Polaris that is required for assembly of the primary cilia in mouse kidney and node (Haycraft et al., 2001; Murcia et al., 2000; Qin et al., 2001; Pazour et al., 2000; Pazour et al., 2002). Thus, IFT involves conserved proteins in many different organisms and plays fundamental roles in a variety of physiological functions. The conservation of function of the two invertebrate homologous genes as essential regulators of sensory ciliogenesis will allow a fruitful comparative identification of novel target genes likely to be involved in IFT.

In *C. elegans*, the only ciliated cells are the sensory neurons; sperm cells are not flagellated and do not express *daf-19*. Conversely, in *Drosophila*, spermatozoids have an unusually long flagella. Interestingly, *Rfx* is also expressed in spermatids but after flagellar elongation during a stage in which only a few genes have been reported to be transcribed (Bendena et al.,

1991; Vandaele et al., 2001), suggesting a different role in spermatogenesis. *Rfx* mutant sperm are normally elongated and motile, and preliminary electron microscopy data show no gross defects in spermatid flagellar 9+2 ultrastructure (not shown). Because *Rfx* mutants are too uncoordinated to mate, we do not know if mutant spermatozoids are functional in fertilization. *Rfx* may have a function in spermatogenesis other than ciliary assembly. This would imply a different mode of flagellar assembly in *Drosophila* spermatozoids that could reflect structural and functional differences between sensory cilia and sperm flagella. *Rfx* is also expressed in subdomain-specific regions of the brain. To our knowledge, no ciliated cells have been described in *Drosophila* brain at the present time, whereas ciliated cells are present in mammalian brain. Studying *Rfx* function in *Drosophila* will thus bring important information regarding the diversification of the function of RFX transcription factors in evolution. Whether the ciliary function of *RFX* genes has been conserved in vertebrates remains an unanswered question and is of great interest regarding human pathologies associated with cilium defects.

This work was supported by grants from the Région Rhône-Alpes (Emergence), the French Ministère de la Recherche (ACI Biologie du développement), from the Association pour la Recherche sur le Cancer and from the Centre National de la Recherche Scientifique. C. V. and R. D. were supported by a doctoral fellowship from the MENRT. A. L. was supported by a postdoctoral fellowship from the Association pour la Recherche sur le Cancer. This work benefited from the technical assistance of J. Schmitt. Electronic microscopy observations were performed with the help of M. Malbouyres and A. Rivoire at the CTμ of the University Claude Bernard. We are grateful to W. Reith who discovered the first RFX genes and with whom this project was initiated. We would also like to thank the members of the Kernan laboratory for helpful discussions. Work in the Kernan laboratory was supported by a fellowship from the Japan Society for the Promotion of Science to E. Shishido and by grants from the National Institute for Deafness and Communicative Disorders and the Pew Scholars Program in the Biomedical Sciences. P. Swoboda was supported by a grant from the Swedish Foundation for Strategic Research (SSF) and thanks J. H. Thomas for his guidance and support.

REFERENCES

Bendena, W. G., Ayme-Southgate, A., Garbe, J. C. and Pardue, M. L. (1991). Expression of heat-shock locus hsr-omega in nonstressed cells during development in Drosophila melanogaster. *Dev. Biol.* **144**, 65-77.

Cheah, P. Y., Chia, W. and Yang, X. (2000). Jumeaux, a novel Drosophila winged-helix family protein, is required for generating asymmetric sibling neuronal cell fates. *Development* **127**, 3325-3335.

Chung, Y. D., Zhu, J., Han, Y. and Kernan, M. J. (2001). nompA encodes a PNS-specific, ZP domain protein required to connect mechanosensory dendrites to sensory structures. *Neuron* **29**, 415-428.

Cobb, M. (1999). What and how do maggots smell? *Biol. Rev.* **74**, 425-459.

Cole, D. G., Diener, D. R., Himelblau, A. L., Beech, P. L., Fuster, J. C. and Rosenbaum, J. L. (1998). Chlamydomonas kinesin-II-dependent intraflagellar transport (IFT): IFT particles contain proteins required for ciliary assembly in Caenorhabditis elegans sensory neurons. *J. Cell Biol.* **141**, 993-1008.

Collet, J., Spike, C. A., Lundquist, E. A., Shaw, J. E. and Herman, R. K. (1998). Analysis of osm-6, a gene that affects sensory cilium structure and sensory neuron function in Caenorhabditis elegans. *Genetics* **148**, 187-200.

David, J. (1962). A new medium for rearing drosophila in axenic conditions. *Dros. Inf. Ser.* **36**, 128.

Deak, P., Omar, M. M., Saunders, R. D., Pal, M., Komonyi, O., Szidonya, J., Maroy, P., Zhang, Y., Ashburner, M., Benos, P. et al. (1997). P-element insertion alleles of essential genes on the third chromosome of Drosophila melanogaster: correlation of physical and cytogenetic maps in chromosomal region 86E-87F. *Genetics* **147**, 1697-1722.

Desai, C. J., Popova, E. and Zinn, K. (1994). A Drosophila receptor tyrosine phosphatase expressed in the embryonic CNS and larval optic lobes is a member of the set of proteins bearing the 'HRP' carbohydrate epitope. *J. Neurosci.* **14**, 7272-7283.

Durand, B., Vandaele, C., Spencer, D., Pantalacci, S. and Couble, P. (2000). Cloning and characterization of *dRFX*, the *Drosophila* member of the RFX family of transcription factors. *Gene* **246**, 285-293.

Dutcher, S. K. (1995). Flagellar assembly in two hundred and fifty easy-to-follow steps. *Trends Genet.* **11**, 398-404.

Eakin, R. M. (1972). Photochemistry of vision. In *Handbook of Sensory Physiology, Vol. VII/1*, pp. 625-684. Berlin: Springer Verlag.

Eberl, D. F., Hardy, R. W. and Kernan, M. J. (2000). Genetically similar transduction mechanisms for touch and hearing in Drosophila. *J. Neurosci.* **20**, 5981-5988.

Emery, P., Durand, B., Mach, B. and Reith, W. (1996). RFX proteins, a novel family of DNA binding proteins conserved in the eukaryotic kingdom. *Nucleic Acids Res.* **24**, 803-807.

Fabini, G., Freilinger, A., Altmann, F. and Wilson, I. B. (2001). Identification of core alpha 1,3-fucosylated glycans and cloning of the requisite fucosyltransferase cDNA from Drosophila melanogaster. Potential basis of the neural anti-horseadish peroxidase epitope. *J. Biol. Chem.* **276**, 28058-28067.

Gajiwala, K. S., Chen, H., Cornille, F., Roques, B. P., Reith, W., Mach, B. and Burley, S. K. (2000). Structure of the winged-helix protein hRFX1 reveals a new mode of DNA binding. *Nature* **403**, 916-921.

Guo, M., Jan, L. Y. and Jan, Y. N. (1996). Control of daughter cell fates during asymmetric division: interaction of Numb and Notch. *Neuron* **17**, 27-41.

Haycraft, C. J., Swoboda, P., Taulman, P. D., Thomas, J. H. and Yoder, B. K. (2001). The C. elegans homolog of the murine cystic kidney disease gene Tg737 functions in a ciliogenic pathway and is disrupted in osm-5 mutant worms. *Development* **128**, 1493-1505.

Heimbeck, G., Bugnon, V., Gendre, N., Haberlin, C. and Stocker, R. F. (1999). Smell and taste perception in Drosophila melanogaster larva: toxin expression studies in chemosensory neurons. *J. Neurosci.* **19**, 6599-6609.

Huang, M., Zhou, Z. and Elledge, S. J. (1998). The DNA replication and damage checkpoint pathways induce transcription by inhibition of the Crt1 repressor. *Cell* **94**, 595-605.

Jan, L. Y. and Jan, Y. N. (1982). Antibodies to horseradish peroxidase as specific neuronal markers in Drosophila and in grasshopper embryos. *Proc. Natl. Acad. Sci. USA* **79**, 2700-2704.

Jan, Y. N. and Jan, L. Y. (1993). The peripheral nervous system. In *The Development of* Drosophila melanogaster, Vol. II (ed. M. Bate and A. Martinez Arias), pp. 1207-1244. Cold Spring Harbor, NY: Cold Spring Harbor Laboratory Press.

Keil, T. A. (1997). Functional morphology of insect mechanoreceptors. *Microsc. Res. Tech.* **39**, 506-531.

Kernan, M., Cowan, D. and Zuker, C. (1994). Genetic dissection of mechanosensory transduction: mechanoreception-defective mutations of Drosophila. *Neuron* **12**, 1195-1206.

Kozminski, K. G., Johnson, K. A., Forscher, P. and Rosenbaum, J. L. (1993). A motility in the eukaryotic flagellum unrelated to flagellar beating. *Proc. Natl. Acad. Sci. USA* **90**, 5519-5523.

Lilly, M. and Carlson, J. (1990). smellblind: a gene required for Drosophila olfaction. *Genetics* **124**, 293-302.

Luo, L., Liao, Y. J., Jan, L. Y. and Jan, Y. N. (1994). Distinct morphogenetic functions of similar small GTPases: Drosophila Drac1 is involved in axonal outgrowth and myoblast fusion. *Genes Dev.* **8**, 1787-1802.

Mann, H. B. and Whitney, D. R. (1947). On a test of whether one of two random variables is stochastically larger than the other. *Ann. Math. Statist.* **18,** 52-54.

Morotomi-Yano, K., Yano, K., Saito, H., Sun, Z., Iwama, A. and Miki, Y. (2002). Human regulatory factor X 4 (RFX4) is a testis-specific dimeric DNA-binding protein that cooperates with other human RFX members. *J. Biol. Chem.* **277**, 836-842.

Murcia, N. S., Richards, W. G., Yoder, B. K., Mucenski, M. L., Dunlap, J. R. and Woychik, R. P. (2000). The Oak Ridge Polycystic Kidney (orpk) disease gene is required for left-right axis determination. *Development* **127**, 2347-2355.

Nonaka, S., Tanaka, Y., Okada, Y., Takeda, S., Harada, A., Kanai, Y., Kido, M. and Kirokawa, N. (1998). Randomization of left-right

asymmetry due to loss of nodal cilia generating leftward flow of extraembryonic fluid in mice lacking KIF3B motor protein. *Cell* **95**, 829-837.

Orgogozo, V., Schweisguth, F. and Bellaiche, Y. (2001). Lineage, cell polarity and inscuteable function in the peripheral nervous system of the Drosophila embryo. *Development* **128**, 631-643.

Pazour, G. J., Dickert, B. L., Vucica, Y., Seeley, E. S., Rosenbaum, J. L., Witman, G. B. and Cole, D. G. (2000). Chlamydomonas IFT88 and its mouse homologue, polycystic kidney disease gene tg737, are required for assembly of cilia and flagella. *J. Cell Biol.* **151**, 709-718.

Pazour, G. J., Baker, S. A., Deane, J. A., Cole, D. G., Dickert, B. L., Rosenbaum, J. L., Witman, G. B. and Besharse, J. C. (2002). The intraflagellar transport protein, IFT88, is essential for vertebrate photoreceptor assembly and maintenance. *J. Cell Biol.* **157**, 103-114.

Perkins, L. A., Hedgecock, E. M., Thomson, J. N. and Culotti, J. G. (1986). Mutant sensory cilia in the nematode Caenorhabditis elegans. *Dev. Biol.* **117**, 456-487.

Prokopenko, S. N., He, Y., Lu, Y. and Bellen, H. J. (2000). Mutations affecting the development of the peripheral nervous system in Drosophila: a molecular screen for novel proteins. *Genetics* **156**, 1691-1715.

Qin, H., Rosenbaum, J. L. and Barr, M. M. (2001). An autosomal recessive polycystic kidney disease gene homolog is involved in intraflagellar transport in C. elegans ciliated sensory neurons. *Curr. Biol.* **11**, 457-461.

Reith, W., Herrero-Sanchez, C., Kobr, M., Silacci, P., Berte, C., Barras, E., Fey, S. and Mach, B. (1990). MHC class II regulatory factor RFX has a novel DNA binding domain and functionally independant dimerization domain. *Genes Dev.* **4**, 1528-1540.

Reith, W. and Mach, B. (2001). The bare lymphocyte syndrome and the regulation of MHC expression. *Annu. Rev. Immunol.* **19**, 331-373.

Rieckhof, G. E., Casares, F., Ryoo, H. D., Abu-Shaar, M. and Mann, R. S. (1997). Nuclear translocation of extradenticle requires homothorax, which encodes an extradenticle-related homeodomain protein. *Cell* **91**, 171-183.

Rosenbaum, J. L., Cole, D. G. and Diener, D. R. (1999). Intraflagellar transport: the eyes have it. *J. Cell Biol.* **144**, 385-388.

Shiraiwa, T., Nitasaka, E. and Yamazaki, T. (2000). Geko, a novel gene involved in olfaction in Drosophila melanogaster. *J. Neurogenet.* **14**, 145-164.

Snow, P. M., Patel, N. H., Harrelson, A. L. and Goodman, C. S. (1987). Neural-specific carbohydrate moiety shared by many surface glycoproteins in Drosophila and grasshopper embryos. *J. Neurosci.* **7**, 4137-4144.

Spradling, A. C. (1986). P element mediated transformation. In Drosophila*: A Practical Approach* (ed. D. Roberts), pp. 175-189. Oxford: IRL Press.

Starich, T. A., Herman, R. K., Kari, C. K., Yeh, W. H., Schackwitz, W. S., Schuyler, M. W., Collet, J., Thomas, J. H. and Riddle, D. L. (1995). Mutations affecting the chemosensory neurons of Caenorhabditis elegans. *Genetics* **139**, 171-188.

Stephens, R. E. (1995). Ciliogenesis in sea urchin embryos – a subroutine in the program of development. *BioEssays* **17**, 331-340.

Strodicke, M., Karberg, S. and Korge, G. (2000). Domina (Dom), a new Drosophila member of the FKH/WH gene family, affects morphogenesis and is a suppressor of position-effect variegation. *Mech. Dev.* **96**, 67-78.

Sun, B. and Salvaterra, P. M. (1995). Characterization of nervana, a Drosophila melanogaster neuron-specific glycoprotein antigen recognized by anti-horseradish peroxidase antibodies. *J. Neurochem.* **65**, 434-443.

Swoboda, P., Adler, H. T. and Thomas, J. H. (2000). The RFX-type transcription factor DAF-19 regulates sensory neuron cilium formation in C. elegans. *Mol. Cell* **5**, 411-421.

Thurm, U. and Kuppers, J. (1980). Epithelial physiology of insect sensilla. In *Insect Biology in the Future* (ed. M. Locke and D. Smith), pp. 735-763. New York: Academic Press.

Uga, S. and Kuwabara, M. (1965). On the fine structure of the chordotonal sensillum in antenna of Drosophila melanogaster. *J Electron Microsc.* **14**, 173-181.

Vandaele, C., Coulon-Bublex, M., Couble, P. and Durand, B. (2001). Drosophila regulatory factor X is an embryonic type I sensory neuron marker also expressed in spermatids and in the brain of Drosophila. *Mech. Dev.* **103**, 159-162.

Walker, R. G., Willingham, A. T. and Zuker, C. S. (2000). A Drosophila mechanosensory transduction channel. *Science* **287**, 2229-2234.

Wang, X., Sun, B., Yasuyama, K. and Salvaterra, P. M. (1994). Biochemical analysis of proteins recognized by anti-HRP antibodies in Drosophila melanogaster: identification and characterization of neuron specific and male specific glycoproteins. *Insect Biochem. Mol. Biol.* **24**, 233-242.

Wu, S. Y. and McLeod, M. (1995). The sak1+ gene of Schizosaccharomyces pombe encodes an RFX family DNA-binding protein thaht positively regulates cyclic AMP-dependant protein kinase mediated exit from the mitotic cycle. *Mol. Cell. Biol.* **15**, 1479-1488.

Zipursky, S. L., Venkatesh, T. R., Teplow, D. B. and Benzer, S. (1984). Neuronal development in the Drosophila retina: monoclonal antibodies as molecular probes. *Cell* **36**, 15-26.